Multi-Component Modeling for Co-Condensation Systems of Silicon-Based Intermetallic Nanoparticle Synthesis Using Induction Thermal Plasmas

Masaya Shigeta and Takayuki Watanabe

Department of Environmental Chemistry and Engineering, Tokyo Institute of Technology, Yokohama, Japan

Abstract

A multi-component co-condensation model was proposed to clarify the formation mechanisms of silicide nanoparticles in induction thermal plasmas. In Cr-Si and Co-Si systems, Si nuclei are produced and they grow, subsequently the metal vapor condenses on the Si particles. In Mo-Si system, Si condenses on the Mo particles produced earlier. Their composition shows a wide range. In Ti-Si system, both vapors of Si and Ti simultaneously condense on the Si nuclei. The silicon content shows a narrow range.

1. Introduction

Induction thermal plasmas (ITPs) have been utilized for material processes such as nanoparticle synthesis since they have several advantages such as high enthalpy, high chemical reactivity, variable properties, large plasma volume, long residence/reaction time, and high quenching rate [1, 2]. Nowadays, nanoparticles of disilicides are required in industrial fields because they provide high electrical conductivity and heat/oxidation resistance. They are, therefore, expected to be applied for electromagnetic shielding, solar control windows, VLSI electrodes, and so on.

The process of the synthesis is, however, a complicated phenomenon with many controlled parameters, and it includes a co-condensation process with large or small vapor pressure differences of prepared species. Although only a few studies and researches have been conducted concerning the synthesis of silicide nanoparticles using ITPs up to the present [3], the formation mechanism of silicide nanoparticles in ITPs is still poorly understood. Therefore, investigation of the formation mechanism of silicide nanoparticles is intensively important for the precise control of the particle size distributions and stoichiometric compositions.

In the present study, numerical analysis is conducted for the synthesis of silicide nanoparticles in an induction thermal plasma to clarify the formation mechanisms especially for chromium-silicon system, cobalt-silicon system, molybdenum-silicon system, and titanium-silicon system. A multi-component co-condensation model is proposed for the co-condensation processes in silicide nanoparticle formation.

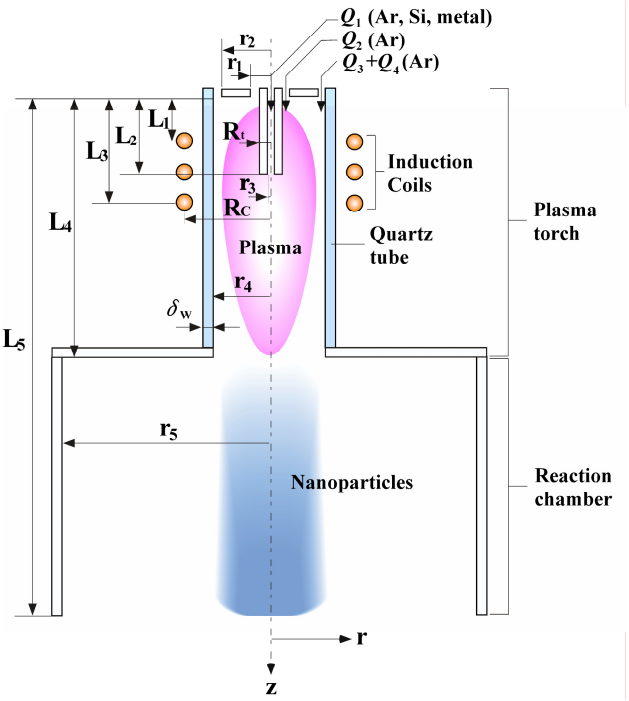

Fig. 1 Nanoparticle synthesis systems.

Table 1 Torch geometry and operating condition.

Torch Power	5 kW
Work Frequency	4 MHz
Reactor Pressure	101.3 kPa
Coil Radius	32 mm
Coil turn number	3
Wall thickness of quartz tube	1.5 mm
Distance to frontal end of coil (L_1)	19 mm
Distance to rear end of coil (L_3)	65 mm
Insertion length of probe (L_2)	45 mm
Torch length (L_4)	190 mm
Outer radius of inner slot (r_1)	6.5 mm
Outer radius of outer slot (r_2)	21 mm
Inner radius of injection tube (r_3)	1 mm
Inner radius of quartz tube (r_4)	22.5 mm
Outer radius of injection tube (R_t)	4.5 mm
Flow rate of carrier gas (Q_1)	0 Sl min^{-1}
Flow rate of plasma gas (Q_2)	3 Sl min^{-1}
Flow rate of plasma gas (Q_3)	10 Sl min^{-1}
Flow rate of sheath gas (Q_4)	20 Sl min^{-1}
Powder feed rate	0.1 g min^{-1}
Silicon content of feed powders	66.7 at%

2. Numerical formulation

Figure 1 shows a schematic illustration of nanoparticle synthesis systems consisting of a plasma torch and a reaction chamber. A summary of the geometry and operating conditions is given in Table 1. Powders of metals and silicon are supplied as the raw materials for silicides with the carrier gas from the central nozzle. The supplied powders are assumed to be vaporized completely due to the high enthalpy of the thermal plasma [3, 4]. The vapors of the metals and silicon are transported with the plasma flow to the reaction chamber and become supersaturated due to the rapid temperature decrease there, which leads to homogeneous nucleation. After homogeneous nucleation, the vapors of metals and silicon co-condense on the nuclei. Silicide nanoparticles are consequently synthesized from the gas phase. The silicon content of the feed powder is chosen to be 66.7 at% considered as the stoichiometric composition of disilicides.

2-1 ITP model

The calculation are based on the following assumptions to derive the governing equations: (a) steady-state laminar flow; (b) axial symmetry; (c) optically thin; (d) negligible viscous dissipation in energy equation; (e) negligible displacement current in comparison with the conductive current; (f) negligible flow-induced electric field; (g) identical temperature of heavy particles and electrons; (h) negligible effects of metals and silicon on thermofluid fields or properties of a plasma.

The fields of flow, temperature and concentration in the induction thermal plasma flow were calculated by solving the two-dimensional continuity, momentum, energy and species conservation equations coupled with the Maxwell's equations. The non-equilibrium effects by the ionization and recombination were taken into account.

Continuity:

$$\nabla \cdot (\rho \boldsymbol{u}) = 0 \tag{1}$$

Momentum:

$$\rho \boldsymbol{u} \cdot \nabla \boldsymbol{u} = -\nabla p + \nabla \tau + \boldsymbol{J} \times \boldsymbol{B} \tag{2}$$

Energy:

$$\rho \boldsymbol{u} \cdot \nabla h = \nabla \cdot \left(\frac{\lambda}{C_p} \nabla h \right) + \boldsymbol{J} \cdot \boldsymbol{E} - q_r \tag{3}$$

Species:

$$\rho \boldsymbol{u} \cdot \nabla Y = \nabla \cdot (\rho D \nabla Y) + R_r \tag{4}$$

Electromagnetic:

$$\nabla^2 \boldsymbol{E} - \xi \sigma_e \frac{\partial \boldsymbol{E}}{\partial t} = 0 \tag{5}$$

The boundary conditions along the centerline were set to insure axial symmetry. At the wall of the plasma torch, no slip conditions are maintained for the velocity, and the concentrations have zero gradient. The temperature at the inside wall of the plasma torch was calculated assuming that the outside wall was maintained at 300 K by water cooling. The injection tube was assumed to be at 500 K. The outflow boundary conditions at the torch were assumed that the gradient of the variables are zero. The sheath gas has swirl velocity component. Each gas stream has constant axial velocity with zero radial velocity having temperature at 300 K. Reaction kinetic rates of the dissociation and recombination as well as the ionization were taken into account. The transport properties were estimated using higher-order approximation of Chapman-Enskog method [5].

The governing conservation equations were solved using SIMPLER (Semi-Implicit Method for Pressure Linked Equation Revised) algorithm [6]. The governing equations and the electric field intensity equation with the associated boundary conditions were discretized into finite difference form using control-volume technique. Non-uniform grid points 30 by 30 were used for radial and axial directions, respectively. Grids were made finer close to the center and the coil region. Thermodynamic and transport properties were calculated from the temperature and compositions at each position in the calculation domain at each iteration step.

2-2 Multi-component co-condensation model

A one-dimensional multi-component model is proposed to clarify the formation mechanism of silicide nanoparticles with the following assumptions: (a) spherical particles; (b) negligible particle inertia due to the small size; (c) the same velocity of the condensing phase and the condensed phase as that of the plasma gas; (d) the same temperature of the nanoparticles as that of the plasma gas; (e) negligible heat generation caused by condensation; (f) the vapors of the metal and silicon considered as ideal gases; (g) negligible agglomeration among the nanoparticles; (h) atmospheric pressure in the systems.

Supersaturated vapor creates nuclei with the critical diameter by homogeneous nucleation [7], subsequently vapors condense heterogeneously on the nuclei [8], which results in nanoparticle growth.

Homogeneous nucleation rate of the species *i*:

$$J_i = \frac{(\beta_{11})_i n_{si}^2 S_i}{12}\sqrt{\frac{\Theta_i}{2\pi}}\exp\left(\Theta_i - \frac{4\Theta_i^3}{27(\ln S_i)^2}\right) \tag{6}$$

Critical diameter:

$$d_{pcri} = \frac{4\sigma_i v_{mi}}{k_B T \ln S_i} \tag{7}$$

Particle growth rate by heterogeneous condensation:

$$\frac{d(d_{pi})}{dt} = \sum_j \alpha_{ij}\frac{4\rho_g}{d_{pi}\rho_{cj}} D_j (X_j - X_j^s)\left\{\frac{1+Kn_i}{1+1.7Kn_i+1.333Kn_i^2}\right\} \tag{8}$$

In Eq. (6), the normalized surface tension Θ and the collision frequency function between a-mer and b-mer β_{ab} can be written as

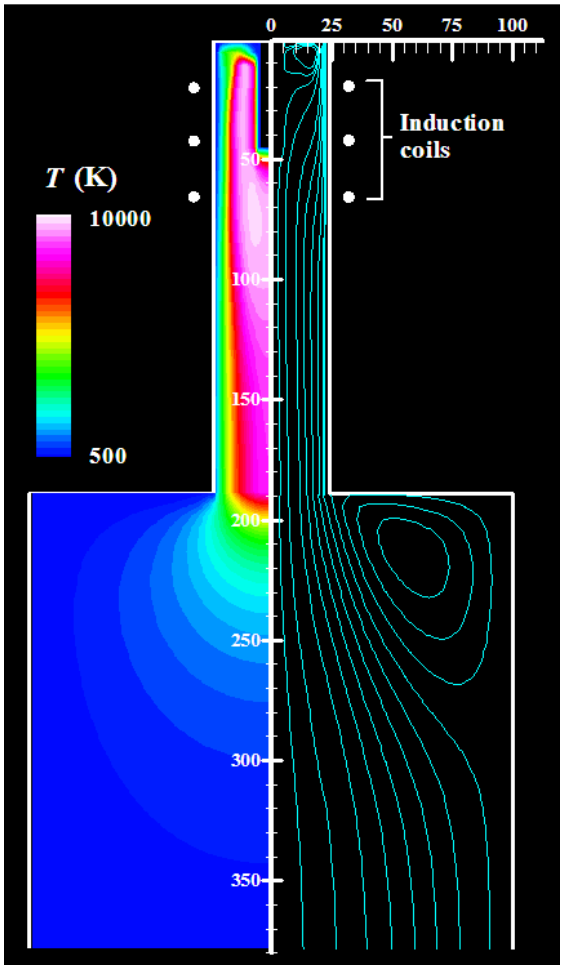

Fig. 2 Temperature (left), streamlines (right).

$$\Theta_i = \frac{\sigma_i s_{1i}}{k_B T} \tag{9}$$

$$\beta_{ab} = \left(\frac{3v_1}{4\pi}\right)^{1/6}\sqrt{\frac{6k_B T}{\rho}\left(\frac{1}{a}+\frac{1}{b}\right)}\left(a^{1/3}+b^{1/3}\right)^2 \tag{10}$$

The concentration of the metal and silicon vapors in the reaction chamber is obtained from the conservation equation written as

$$\rho u\frac{\partial c_i}{\partial z} = -G_i \tag{11}$$

The very fine computation grids are required for the nanoparticle synthesis since the nucleation and condensation processes have much smaller characteristic times than the plasma flow. Thus the grids of the reaction chamber (z=190-380 mm) are divided in 5,000 uniform grids in z-direction for the nanoparticle synthesis. The data obtained by the computation of the plasma such as the temperature and the velocity are modified for the fine grid system to calculate the rates of nucleation and condensation.

3. Results and discussion

Figure 2 shows the thermofluid fields in the plasma torch and the reaction chamber. The Joule heating by the applied electromagnetic power generates the remarkably high temperature zone (higher than 9,500 K) in and below the coil region. The high enthalpy of the plasma is

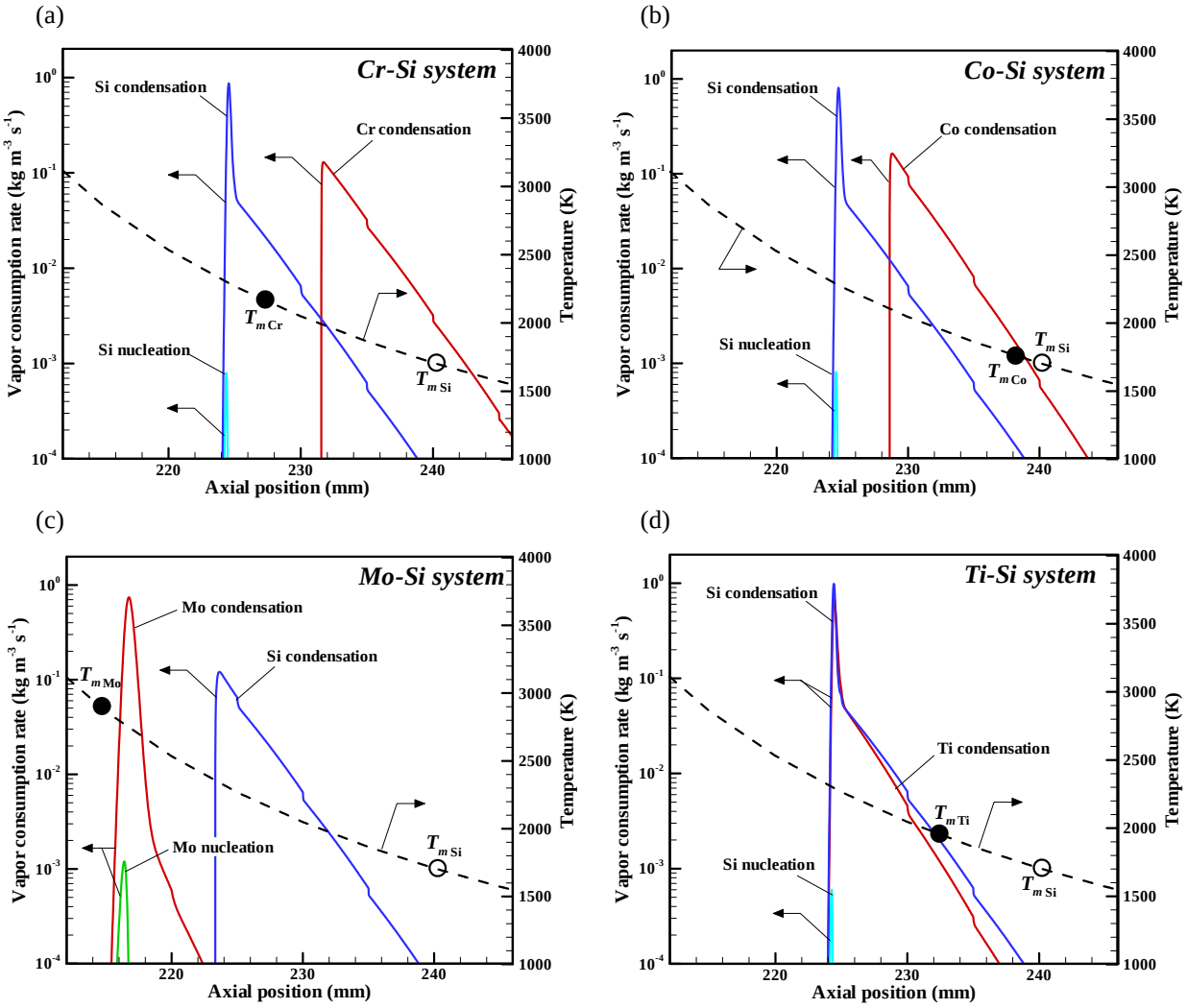

Fig. 3 Axial evolution of vapor consumption rate:
(a) Cr-Si system, (b) Co-Si system, (c) Mo-Si system, and (d) Ti-Si system

transported to the downstream region by the convection. The characteristic recirculation flow exists above the coil region since the radial Lorentz force induced in the plasma pinches the flow. In the reaction chamber, the temperature decreases drastically to below 500 K. As the result, the high quenching rate (10^4-10^5 K s^{-1}) is obtained, which leads to considerable promotion of particle nucleation.

Figures 3 (a)-(d) show the axial evolutions of the vapor consumption rate. In Cr-Si system, silicon vapor is consumed by the particle growth with homogeneous nucleation and heterogeneous condensation at the more upstream position than chromium vapor. At the downstream position, the chromium vapor consumption occurs by heterogeneous condensation on silicon particles. When chromium vapor condenses on the silicon particles, chromium is considered to be well-mixed in the liquid silicon particles with the particle growth since the temperature is higher than the melting temperature of silicon. Therefore, the nanoparticles of chromium-silicides are well-synthesized. In Co-Si system, it shows the same tendency as Cr-Si system. The cobalt vapor consumption by condensation occurs at the more upstream position compared with Cr-Si system as shown in Fig. 3 (a) since the saturation pressure of cobalt is smaller than that of chromium.

In Mo-Si system, molybdenum particles grow by homogeneous nucleation and heterogeneous condensation, subsequently silicon vapor condenses on the molybdenum particles. The temperature of the nanoparticle growth region is lower than the melting point of molybdenum. This indicates poor synthesis of silicides, because molybdenum and silicon should be well-mixed to form silicides in the condensation process. However, the stoichiometric compounds of molybdenum-silicides were observed in the experimental study [3]. The nanoparticles are, therefore, considered to grow in a super-cooled liquid state as the mixture of molybdenum and silicon even at the lower temperature than the melting point of

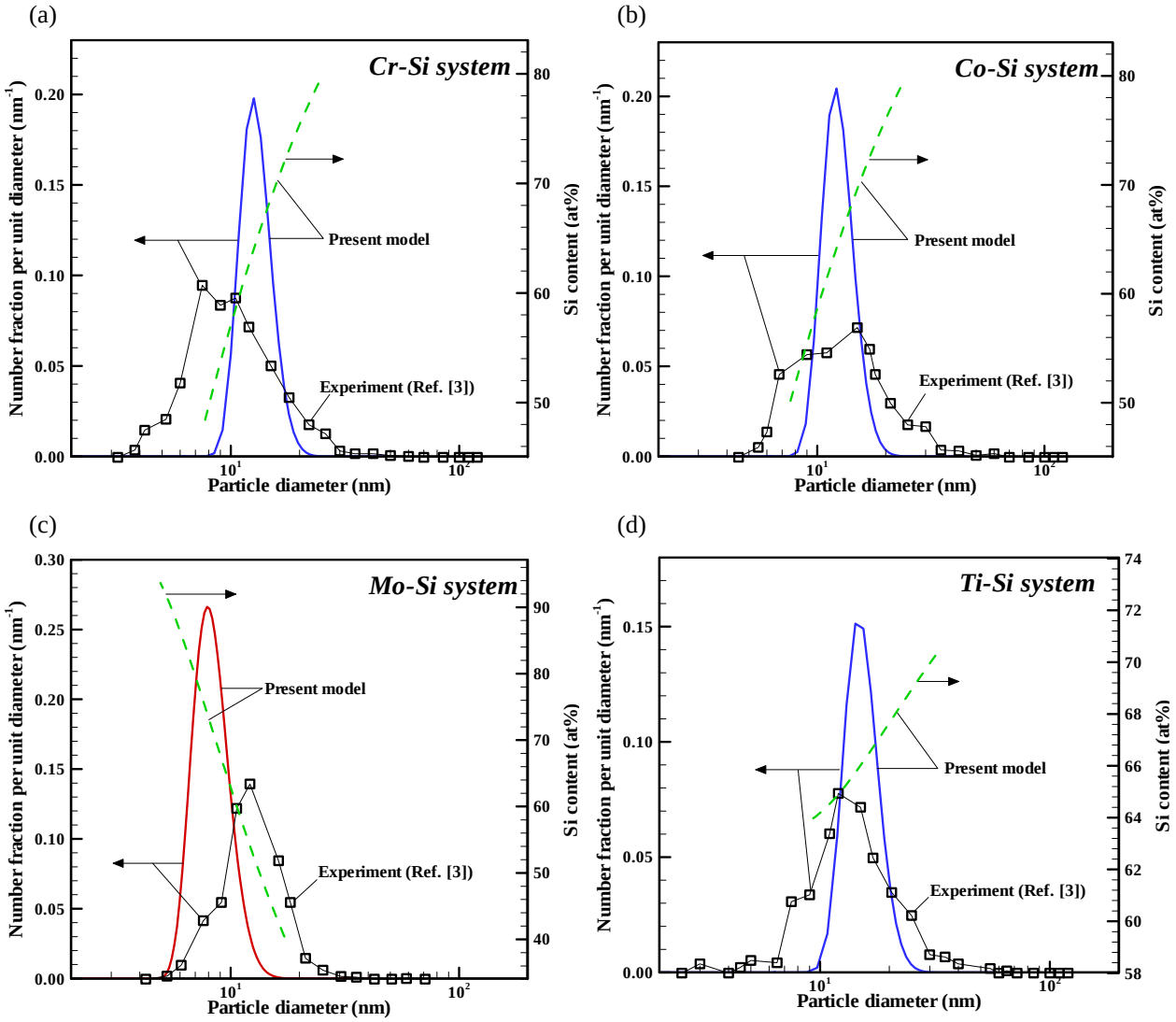

Fig. 4 Particle size distribution and silicon content:
(a) Cr-Si system, (b) Co-Si system, (c) Mo-Si system, and (d) Ti-Si system

molybdenum by the high quenching rate at the tail of the induction thermal plasma.

In Ti-Si system, silicon nucleates earlier than titanium. Immediately after the nucleation of silicon, the vapors of silicon and titanium are simultaneously consumed by heterogeneous condensation. Silicon and titanium are considered to be well-mixed in a liquid state in this co-condensation process since the particles grow at the temperature higher than the melting points of titanium and silicon, which results in the better synthesis of titanium-silicides.

Figures 4 (a)-(d) show the particle size distributions and the silicon contents finally obtained by the present model for four systems. The number mean diameters are 13.3 nm in Cr-Si system, 12.8 nm in Co-Si system, 8.5 nm in Mo-Si system, and 15.8 nm in Ti-Si system. Mo-Si system produces smaller nanoparticles than the other systems due to the difference of the nucleus size. Molybdenum nucleates with the smaller critical diameters from 0.59 to 1.94 nm, while the critical diameters of the silicon nuclei in other systems show from 0.83 to 2.65 nm. Since a larger number of the smaller nuclei are produced in Mo-Si system, a smaller amount of the vapors is consumed per one nucleus for the particle growth. As the result, the obtained particle diameters in Mo-Si system show smaller than those in the other systems. In all systems, the particle size distributions agree well with the experimental results [3].

The silicon contents show some ranges along with the particle diameters. Cr-Si system and Co-Si system have a range 48.1-79.4 at% and 49.5-79.3 at%, respectively. Mo-Si system particularly has a wide range 40-94 at%. Only Ti-Si system has a narrow range 64-70 at%, which results in the more homogeneous synthesis of the disilicide. These are determined by the balance of the contents of the formerly produced

Table 2 Compositions estimated from Ref. [9]

System	Main product	Sub-product
Cr-Si	$CrSi_2$	Cr_5Si_3, CrSi, Si
Co-Si	$CoSi_2$	CoSi, Si
Mo-Si	$MoSi_2$	Mo_5Si_3, Si
Ti-Si	$TiSi_2$	TiSi, Si

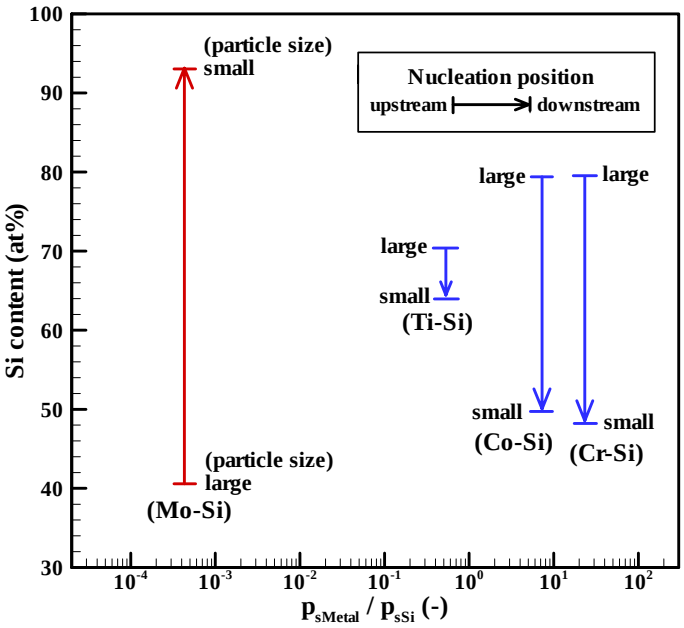

Fig. 5 Correlation chart between saturation pressure ratio and silicon content.

nuclei and the following condensing vapor. This indicates that the silicide nanoparticles synthesized in the induction thermal plasma provide diverse compositions. The compositions of the products can be estimated from the obtained silicon contents by comparing with the phase diagrams of silicides [9] and summarized in Table 2. In all systems, the required disilicides are synthesized as the main products, while the sub-products are synthesized as well, even though the powders of the raw materials are supplied with the stoichiometric compositions of the disilicides. This is because the condensation positions are different due to the different vapor pressures of the materials. However, induction thermal plasmas with the high enthalpy and the high quenching rate are notably effective even for the difficult co-condensation processes with the large vapor pressure differences. These results about the composition of the synthesized silicide nanoparticles obtained from the present model also show good agreements with the experiment [3].

Figure 5 is the correlation chart between the saturation pressure ratios and the silicon contents at the nucleation positions obtained from the present study. The larger particles with silicon nuclei generated at the upstream positions provide the larger silicon contents in Cr-Si system, Co-Si system, and Ti-Si system, while the smaller particles with molybdenum nuclei generated at the downstream positions provide the larger silicon contents in Mo-Si system. Furthermore, the silicon contents show the wide ranges when condensations of metal and silicon occur at the different positions due to the largely different vapor pressures as shown in Cr-Si system, Co-Si system, and Mo-Si system. The silicon content shows the particularly narrow range when condensations of metal and silicon occur simultaneously as shown in Ti-Si system.

This chart indicates that processes including large difference of the saturation pressures between the metal and silicon tend to produce silicide nanoparticles with wide range of composition. Conversely, the composition of the nanoparticles can be evaluated from the ratio of the saturation pressures between the metal and silicon. This chart can be used for prediction of composition in the co-condensation process.

References

[1] T. Watanabe, A. Nezu, Y. Abe, Y. Ishii, K. Adachi - Thin Solid Films 435, 27 (2003).
[2] M. Shigeta, T. Watanabe, H. Nishiyama - Thin Solid Films 457, 192 (2004).
[3] T. Watanabe, H. Okumiya - Sci. and Tech. of Advanced Materials 5, 639 (2004).
[4] M. Shigeta, T. Sato, H. Nishiyama - Int. J. Heat and Mass Transfer 47, 707 (2004).
[5] J. O. Hirschfelder, C. F. Curtiss, R. B. Bird - Molecular Theory of Gases and Liquids (John Wiley, New York, 1964).
[6] S.V. Patankar - Numerical Fluid Flow and Heat Transfer, 138 (Hemisphere, New York, 1980).
[7] S.L. Girshick, C.P. Chiu, P.H. McMurry - Aerosol Sci. and Tech. 13, 465 (1990).
[8] S.V. Joshi, Q. Liang, J.Y. Park, J.A. Batdorf - Plasma Chem. Plasma Proc. 10-2, 339 (1990).
[9] T.B. Massalski - Binary Alloy Phase Diagrams. 2nd Ed. 3, 2664 (American Society for Metals, Materials Park, 1990).